

## FABRICATION AND PRESSURIZATIONS TECHNOLOGY FOR IMPROVEMENT OF SURFACE ACCURACY OF PASSIVE COMMUNICATIONS SATELLITES

By David C. Grana and Walter E. Bressette

NASA Langley Research Center

### INTRODUCTION

Since the successful demonstration of the Echo I satellite for the purpose of communication by means of passive reflecting of radio waves, the NASA Langley Research Center through both in-house and contractual studies by the G. T. Schjeldahl Company of Northfield, Minnesota, has been actively engaged in a research program to improve the RF reflecting surface of the passive communication satellite.

The objectives of the program are first to investigate and document the state-of-the-art fabrication technique used for the Echo satellites in order to establish the source and magnitude of the inherent errors during forming, cutting, sealing, and handling; second, to evaluate improved manufacturing procedures by constructions of small-scale 12-foot spheres using such devices as mandrels and molds; and, third, to determine the effects of the number of gores and the manufacturing process on the surface conditions and radius of curvature accuracy before, during, and after internal 12-foot-diameter-sphere pressurization using a photogrammetry technique. This paper will present the highlights of this program.

### CONCEPT AND THEORY

The Echo concept illustrated in figure 1 is, in fact, an approximate sphere consisting of a number of flat gores, fastened together by 1-inch-wide adhesive-coated tapes, with spherically shaped caps located at both ends of the gores. The shape and size of the gore are determined by a geometric projection (ref. 1) with the edges of the gores representing great circles on the flat-sided approximate sphere. The greater the number of gores the closer the flat-sided figure will approximate a sphere. The entire structure is made of a pliable material, which, after deployment in space, is presumed permanently strained by an inflatant to form a rigid spherical shape with the center line of the gore  $L$  permanently yielded to equal the gore edge line  $C$ . The degree of permanent strain required is illustrated in figure 2. The plot shows that the permanent strain required to strain a gore-constructed approximate sphere to spherical shape is only dependent upon the number of gores in the sphere and is reduced as the number of gores is increased. The curve was calculated from the equation shown on the right side of the figure.

1. Wellman, B. Leighton: Technical Descriptive Geometry. McGraw-Hill Book Co., Inc., 1948.

$$\epsilon_p = \frac{\frac{\pi}{N} - \sin \frac{\pi}{N}}{\sin \frac{\pi}{N}} \quad (1)$$

where

$\epsilon_p$  permanent strain required to obtain a perfect sphere

N number of gores in approximate sphere

The equation was derived from the concept illustrated in the sketch representing a cross section of one of the gores in the approximate sphere where the objective in pressurizing the balloon is to yield the material from the flat chord section, as shown by the dotted line, to a spherical arc contour, as shown by the curved line.

The permanent strain may next be related to the skin stress by means of the stress-strain curve for the material under consideration. For the present application, Echo II material was used, mainly because of material availability and the possibility of comparing the final 12-foot-diameter test spheres with much larger sphere data. An Instron stress-strain curve for the Echo II material is presented on the left in figure 3. In order to be sure if the uniaxial Instron data would be realistic for predicting the stress required for the approximate spheres, additional stress-strain information was obtained by a diaphragm technique that stressed the material biaxially. As can be seen, the diaphragm data agree quite well with the continuous and much easier to obtain Instron data. From the Instron stress-strain curve the permanent strain was analytically determined and is presented on the right side of the figure. Because of the difficulty of locating multilaminate material yield points necessary for determining the permanent strain from an Instron stress-strain curve, an optical comparator was used to measure the Instron sample before and after stressing to determine the actual permanent strain obtained. These data are also presented in the right-hand plot and compare very well with the analytical data taken from the Instron stress-strain curve. It is now possible, by use of figures 2 and 3 and the thin-wall homogeneous sphere equation, to calculate the internal pressure required to strain an approximate sphere constructed of a specified number of gores to spherical shape. It is conceivable that, even though the sphere is nonhomogeneous, the thin-wall homogeneous sphere equation is valid to predict the point where the flat gore will reach a spherical shape, because the double-thick material at the tapes should not yield appreciably compared to the gore material.

If the perfect sphericity point, at any point on the approximate sphere, is exceeded, then use of the thin-wall sphere equation cannot hope to be valid because of the variation in material thickness throughout the sphere. It also seems realistic that any manufacturing imperfection that must be removed by strain has to be such that will require strains less than the strain necessary to remove the flat gores. In light of this thought, it next became important to determine the manufacturing tolerance for the Echo method of construction. The inherent errors during forming, cutting, and sealing were summed and equated to the gore method of construction as percent of width of gore. Because the calculated errors remained constant and the gore width varied, it became apparent at this point, as shown in figure 4 that the strain required

to remove the maximum expected fabrication errors would vary from pole to equator by as much as a factor of 10 with the pole area requiring the greatest amount of correction. Figure 4 shows the maximum percent error, which is equivalent to maximum strain required to remove the error, for Echo II material and the 12-foot spheres used in this program. The curves were calculated from the equation to the right of the figure.

Equation (1) of figure 4 is the equation for the curve:

$$\text{Percent error} = \frac{k \Sigma(\text{errors})}{\sin \theta} = \frac{100 \Sigma \text{ errors}}{W}$$

where

$$k = \frac{100 \sin \theta}{W}$$

Equation (2) determines the width of the gore

$$W = \frac{2\pi R \sin \theta}{N}$$

where

R     radius of sphere

N     number of gores

It is interesting to note that the 24-gore mandrel-constructed 12-foot-sphere maximum-error curve is very similar to the Echo II 135 sphere curve. It is also evident from the magnitude of the percent error, especially in the sphere pole-cap area, that the actual errors will have to be much less than predicted in order to avoid exceeding the required strain for removal of the flat gores.

## EXPERIMENTAL APPROACH

Since the strain theory was not related to the size of the sphere and the strain requirements for correcting the manufacturing tolerances could not be optimized by theory, a 12-foot sphere was selected for the program test size because it was the largest sphere that could be built practically, handled, and photographed in the numbers required. Nine spheres were built, one or more 32, 48, and 64 flat-gore spheres by the Echo II method which, as shown in figure 5, consisted of seaming together with 1/2-inch-tape, pre-cut gores on a curved rail; three 48 flat-gore spheres where adjacent gores were cut and sealed without gore position change on the mandrel shown in figure 6; and one 48 flat-gore sphere which was constructed on a hemispherical mold. The mold-type construction would not be practical for the large spheres, but

it was included in this program in order to compare manufacturing errors. Photogrammetry measurements of the spheres were made by Ohio State University at low and high pressure for all the spheres, first at a very low pressure to determine the manufactured condition, and, in sequential order, as shown in figure 7, in order to determine the effect pressurization had on the sphericity of the originally constructed sphere. From the initial low value the pressure was increased to one-half the value calculated as the perfect sphericity pressure depending upon the number of gores, back to the low value, next up to the design and back to the low pressure, and then to  $1\frac{1}{2}$  design

before returning to the low pressure again. The photogrammetry plates were then converted to contour plots by a wild A-7 autograph. In figure 8 is shown a typical contour map which covers approximately  $\frac{1}{4}$  the area of the 12-foot-diameter sphere. From contour plots such as this, cross sections along the gore center line, parallel to the gore at the equator and through the pole caps were obtained from which overall changes in sphericity with pressurization could be observed. The wild A-7 autograph is also capable of magnifying local areas of the contour plots for the purpose of observing manufacturing imperfections from which the various techniques of manufacturing will be compared.

## RESULTS AND DISCUSSION

At the present time all of the spheres have been photographed and much of the photogrammetric data is still being analyzed. The detailed manufacturing imperfections from the various methods of manufacturing will be published at a later date. Enough information on the sphericity of the approximate spheres with increasing pressure is available to clearly make some preliminary conclusions.

Presented in figure 9 is the ratio of measured to design radius of curvature along a gore center line and across the gores at the balloon equator before and after pressurization to both design and  $1\frac{1}{2}$  times design for the 32-gore approximate sphere. It can be seen at the initial low pressure that in general the balloon is constructed from 0 to 60 inches from the equator nearly as designed but is poorly constructed from 60 inches to 72 inches from the equator. This is not too surprising since this area, as shown in figure 4, is the same area where the manufacturing errors are increasing very rapidly and also where the gores terminate in a solid one-piece spherical pole cap. It cannot be expected that every balloon constructed of gores would be out of design near the pole cap as much as this one but it is reasonable to say that the pole-cap area is the most critical construction area and as seen from the data at the initial low pressure could be the limiting factor for the overall tolerance on sphericity of the inflatable sphere. In general, the sphericity of the sphere both along a gore and across the gores improves with increasing pressure. However, the pole area fault remained even after the approximate sphere had been stressed to an average pressure of  $1\frac{1}{2}$  times that required to theoretically strain the gores to spherical shape.

## CONCLUDING REMARKS

In summary, from theoretical consideration and experimental data taken by means of photogrammetry on 12-foot-diameter gore-constructed approximate spheres, the following concluding remarks can be made:

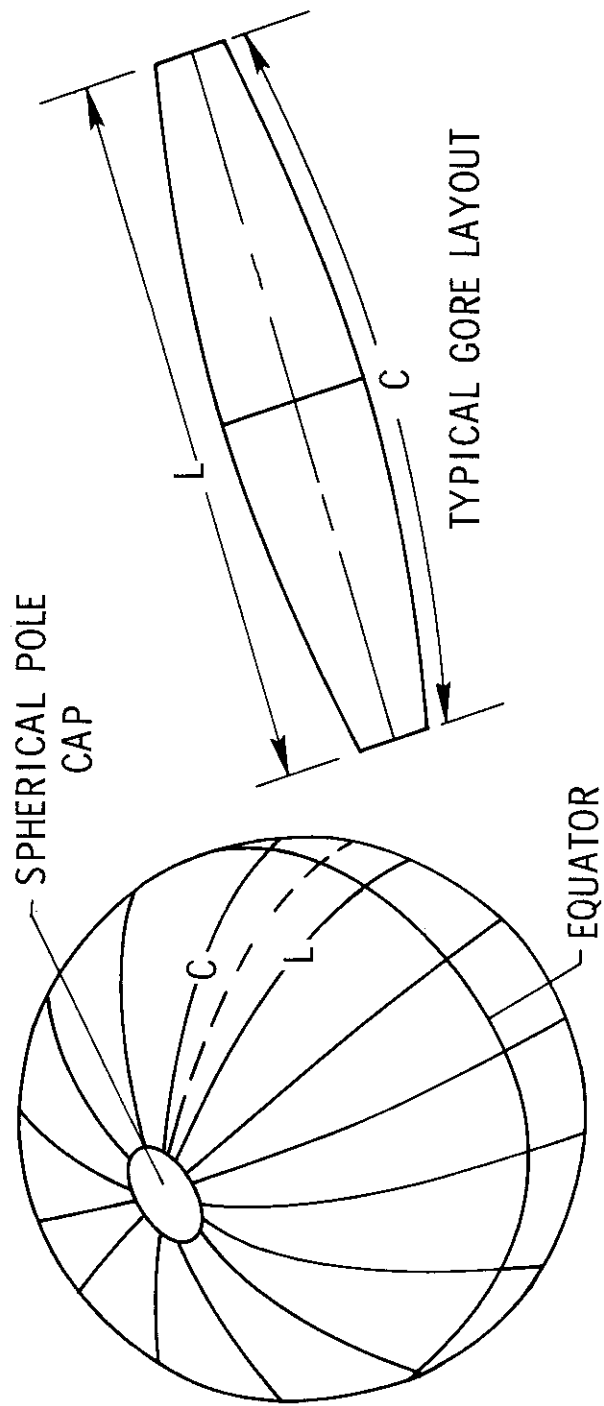
1. The permanent strain required to strain a gore-constructed approximate sphere to spherical shape is only dependent upon the number of gores in the sphere.

2. The greater the number of gores in a gore-constructed approximate sphere, the lower the strain required to strain the approximate configuration to spherical shape by an inflatable system.

3. Stress-strain data obtained by a biaxial diaphragm technique agreed with the continuous and much easier to obtain Instron data.

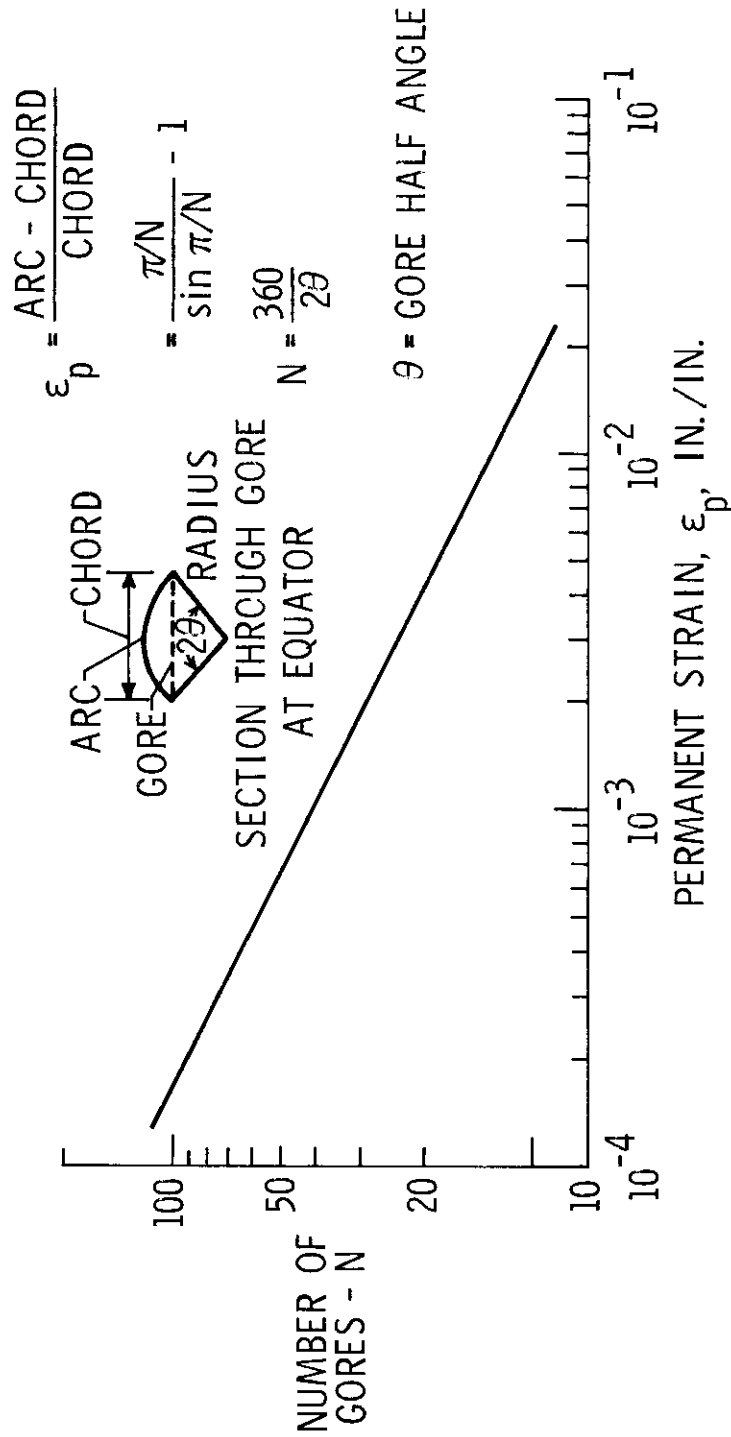
4. The strain required to remove the maximum expected fabrication errors varied from pole to equator by as much as a factor of 10 with the pole area requiring the greatest amount of correction.

5. In general, the sphericity of the 32-gore approximate sphere improved with increasing pressure, but it was not possible to remove a faulty pole-cap area by stressing the balloon to  $1\frac{1}{2}$  times the theoretical pressure required to strain the gores to spherical shape.



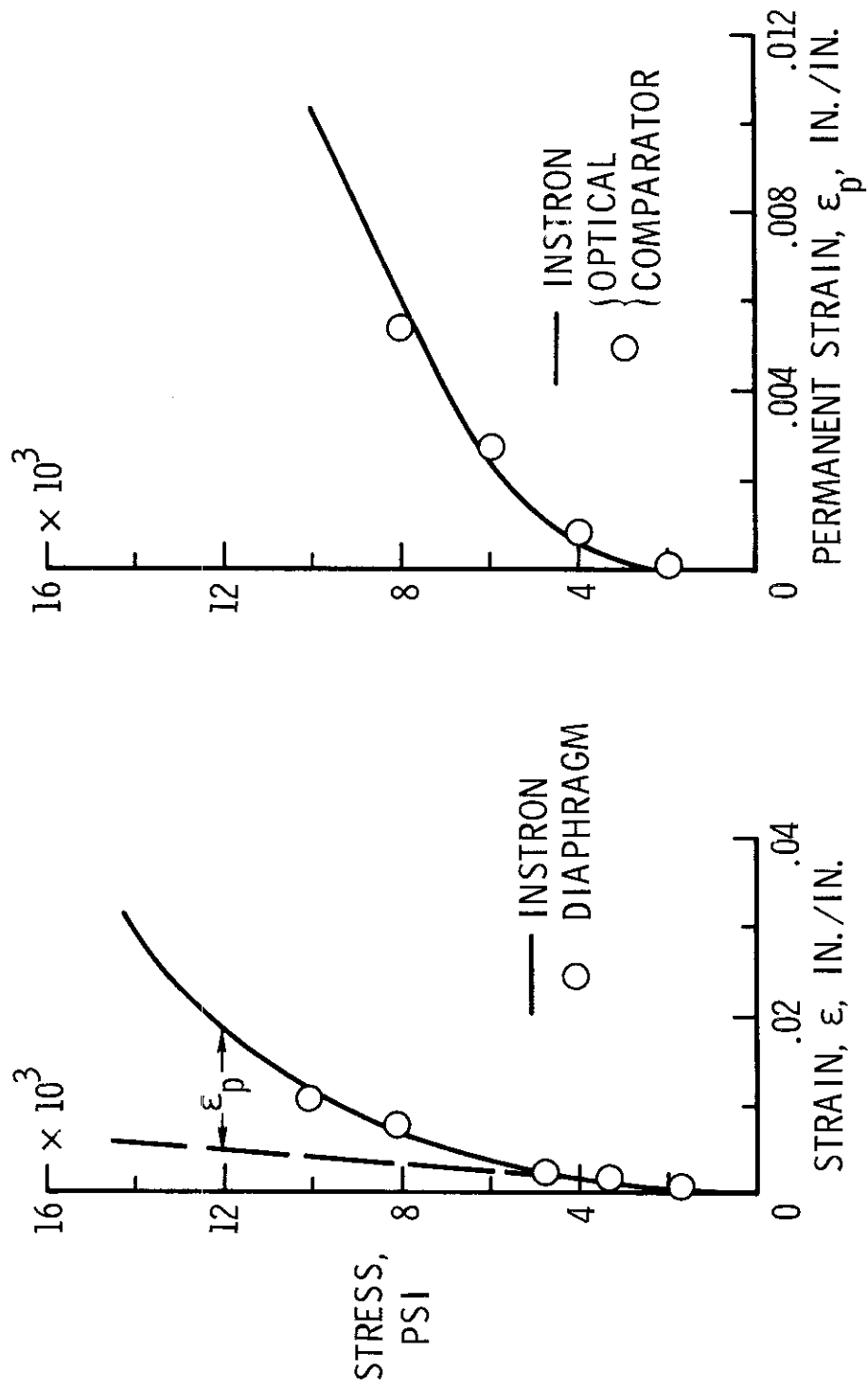
NASA

Figure 1.- Gore construction technique.



NASA

Figure 2.- Permanent strain requirements as a function of number of gores.



NASA

Figure 3.- Stress/strain data for Echo II material.



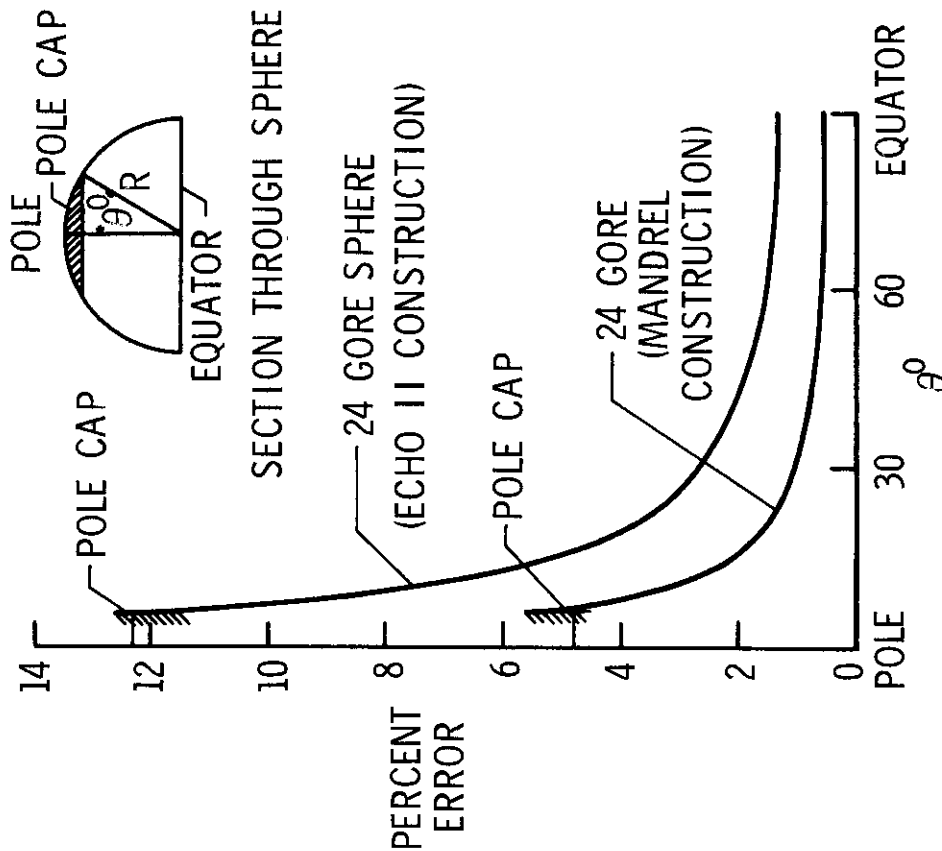


Figure 4.- Variation in maximum error due to fabrication imperfections as a function of angular location on sphere.

NASA

PERCENT ERRORS

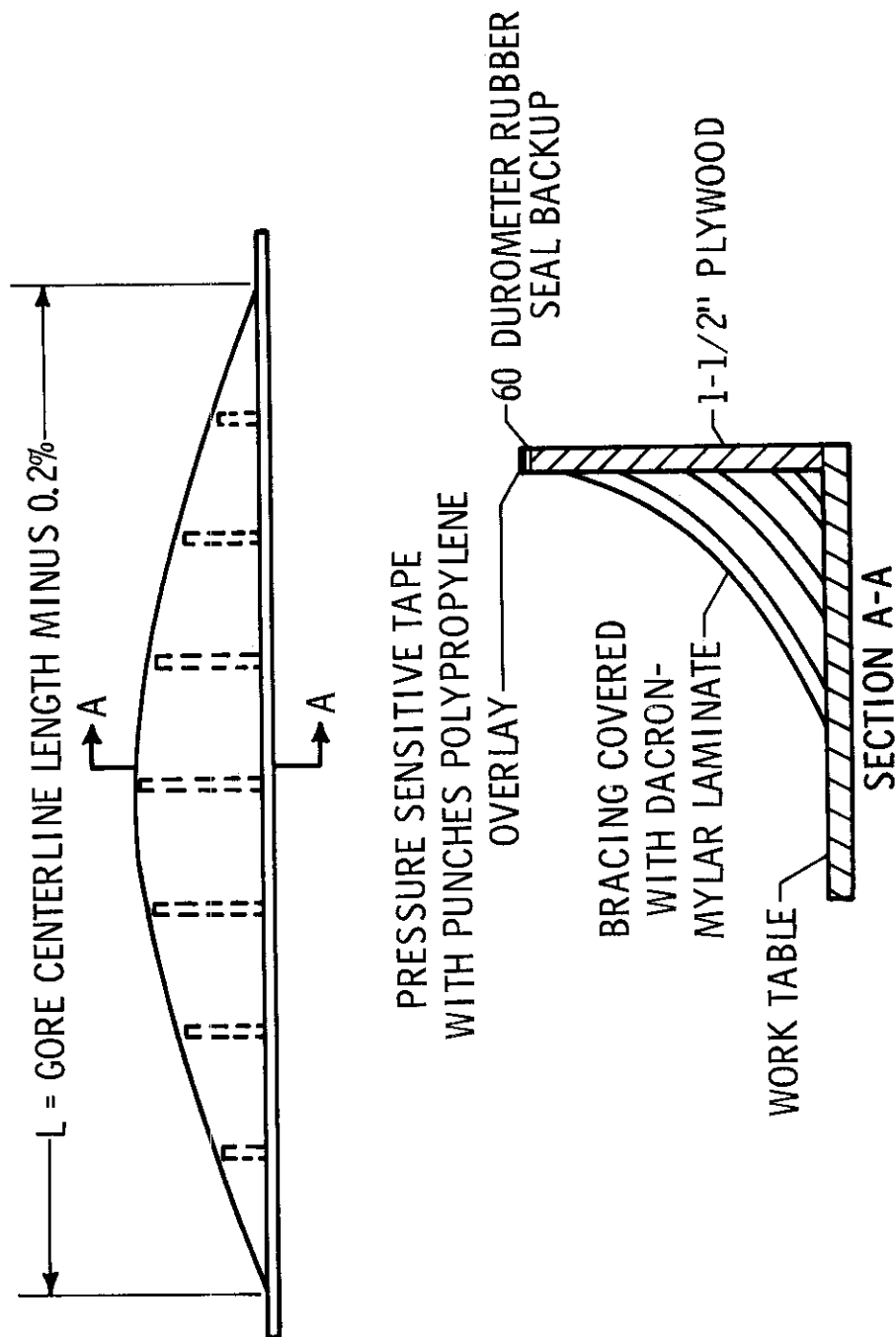
$$= \frac{k \Sigma(\text{ERRORS})}{\sin \theta} \quad (1)$$

$$k = \frac{100 \sin \theta}{W}$$

$$W = \frac{2\pi R \sin \theta}{N} \quad (2)$$

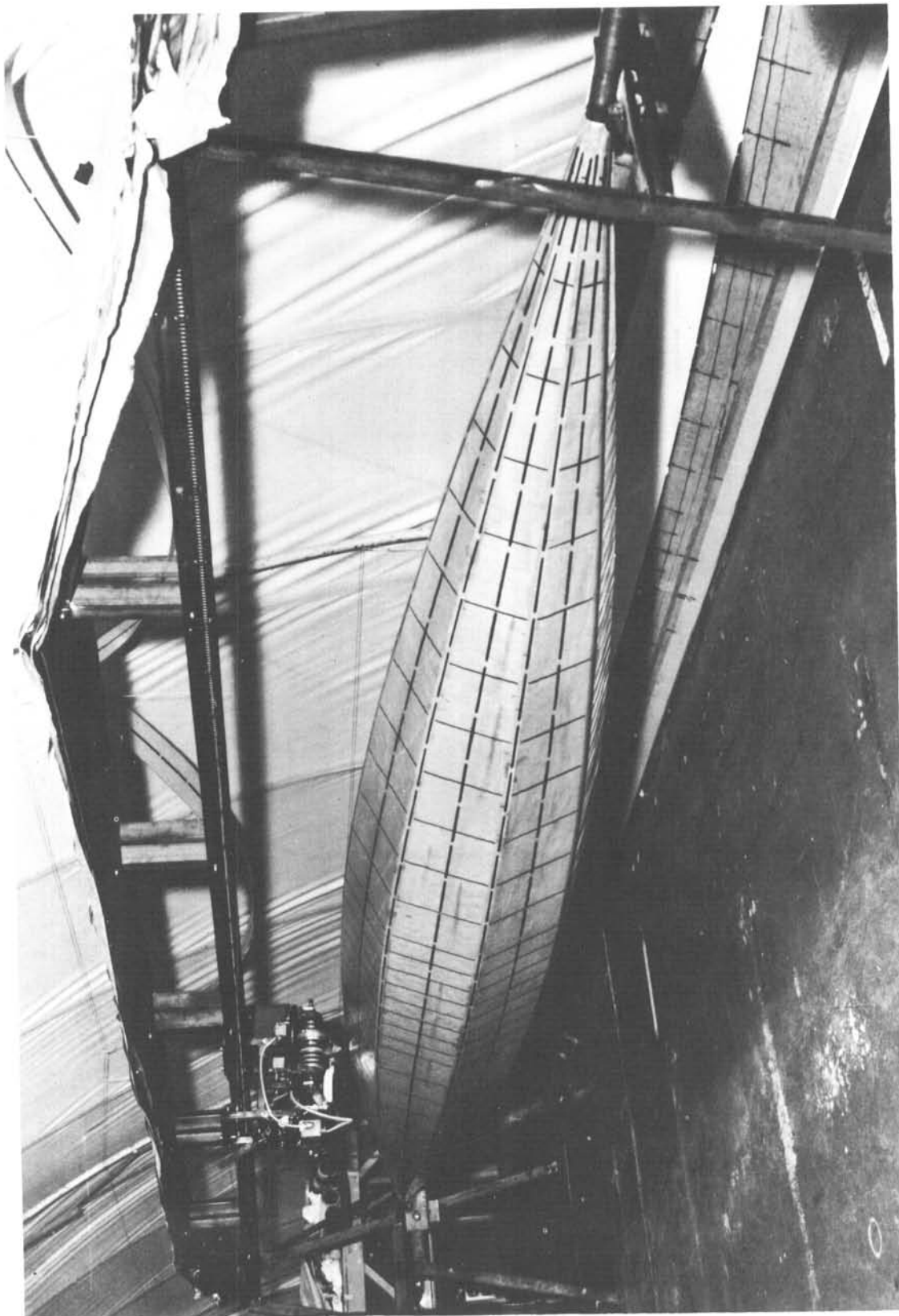
N = NUMBER OF GORES

R = RADIUS



NASA

Figure 5.- Typical sealing rail - 12-foot spheres.



NASA

Figure 6.- Mandrel technique for fabrication of gores.

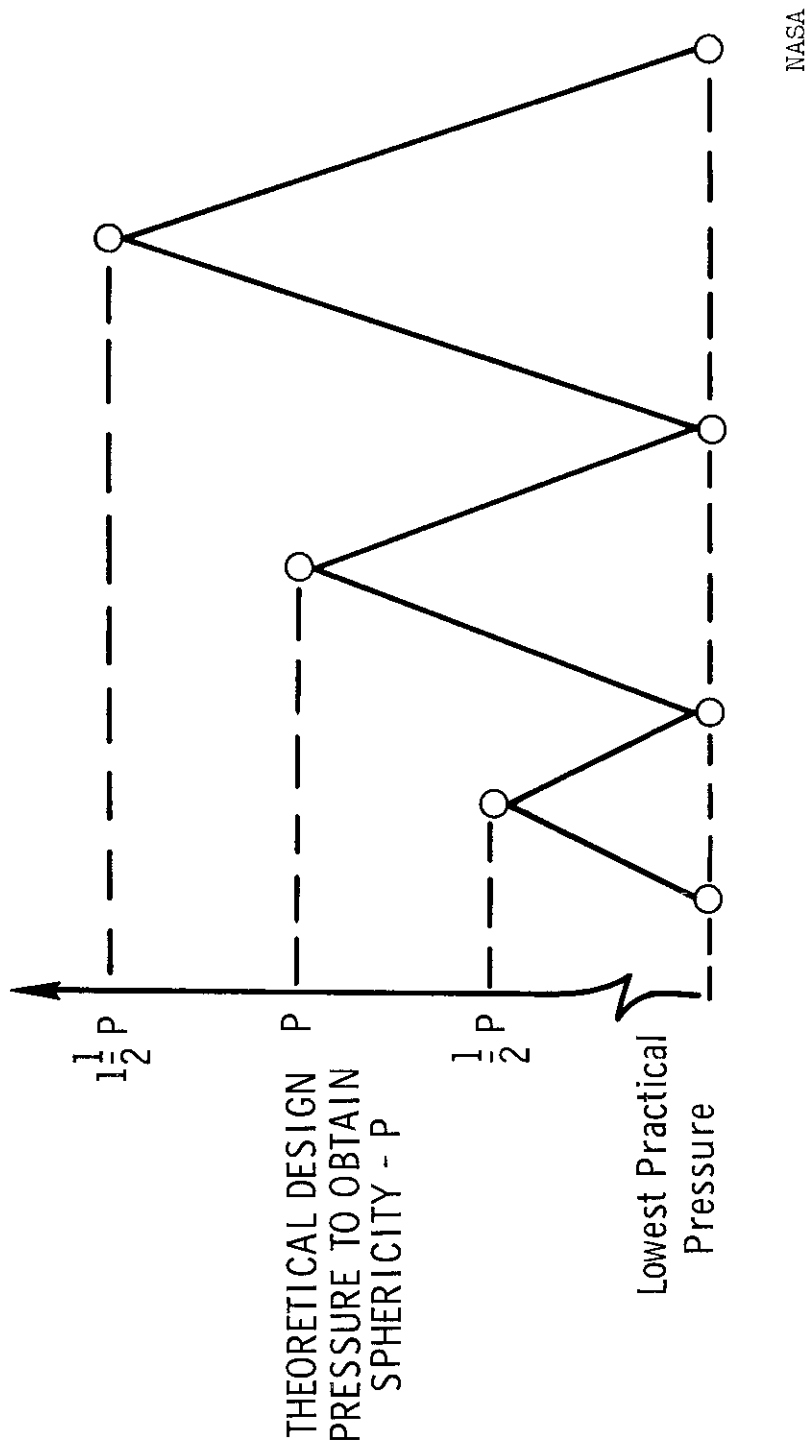


Figure 7.- Techniques used to inflate and measure test spheres.

NASA

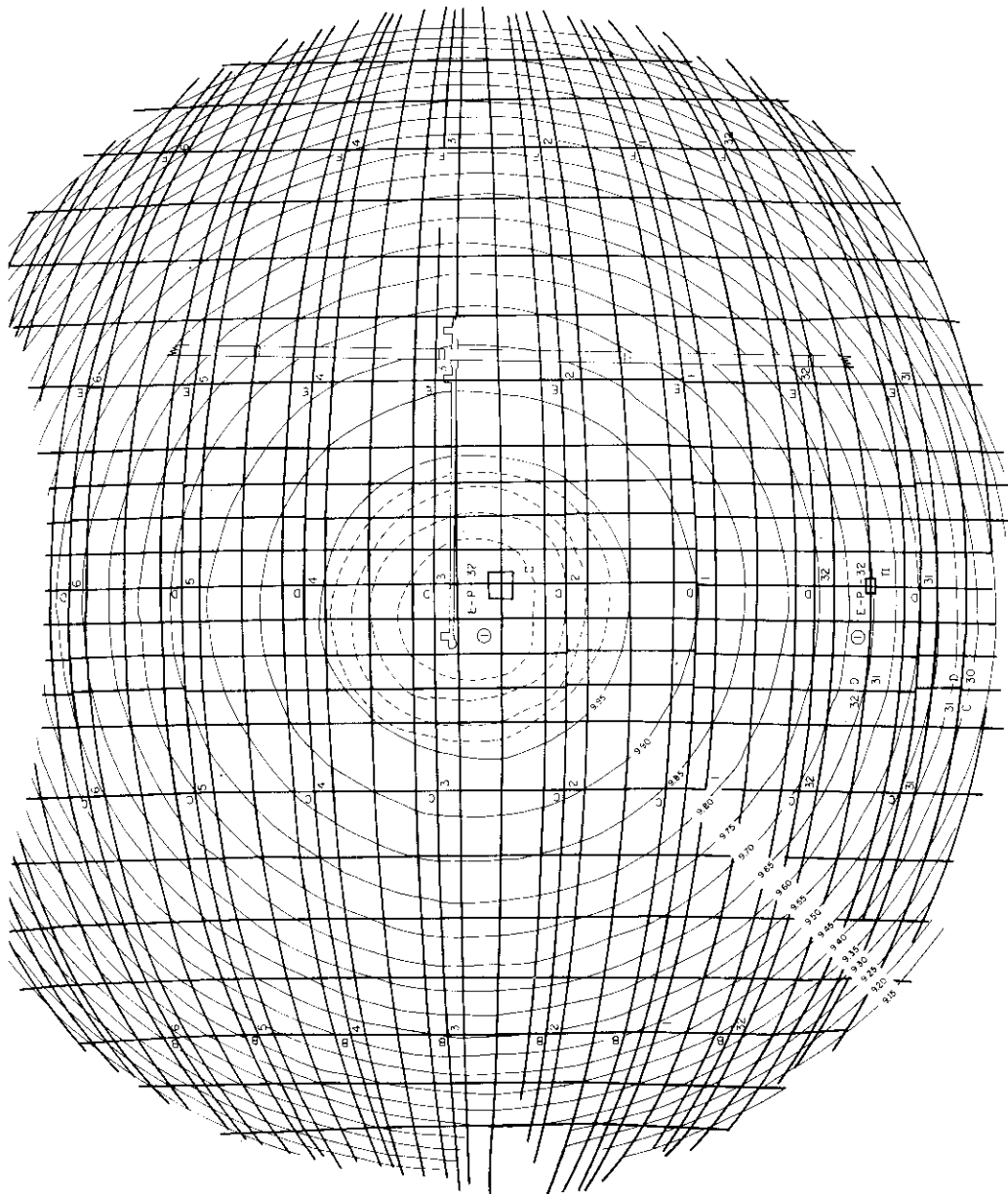
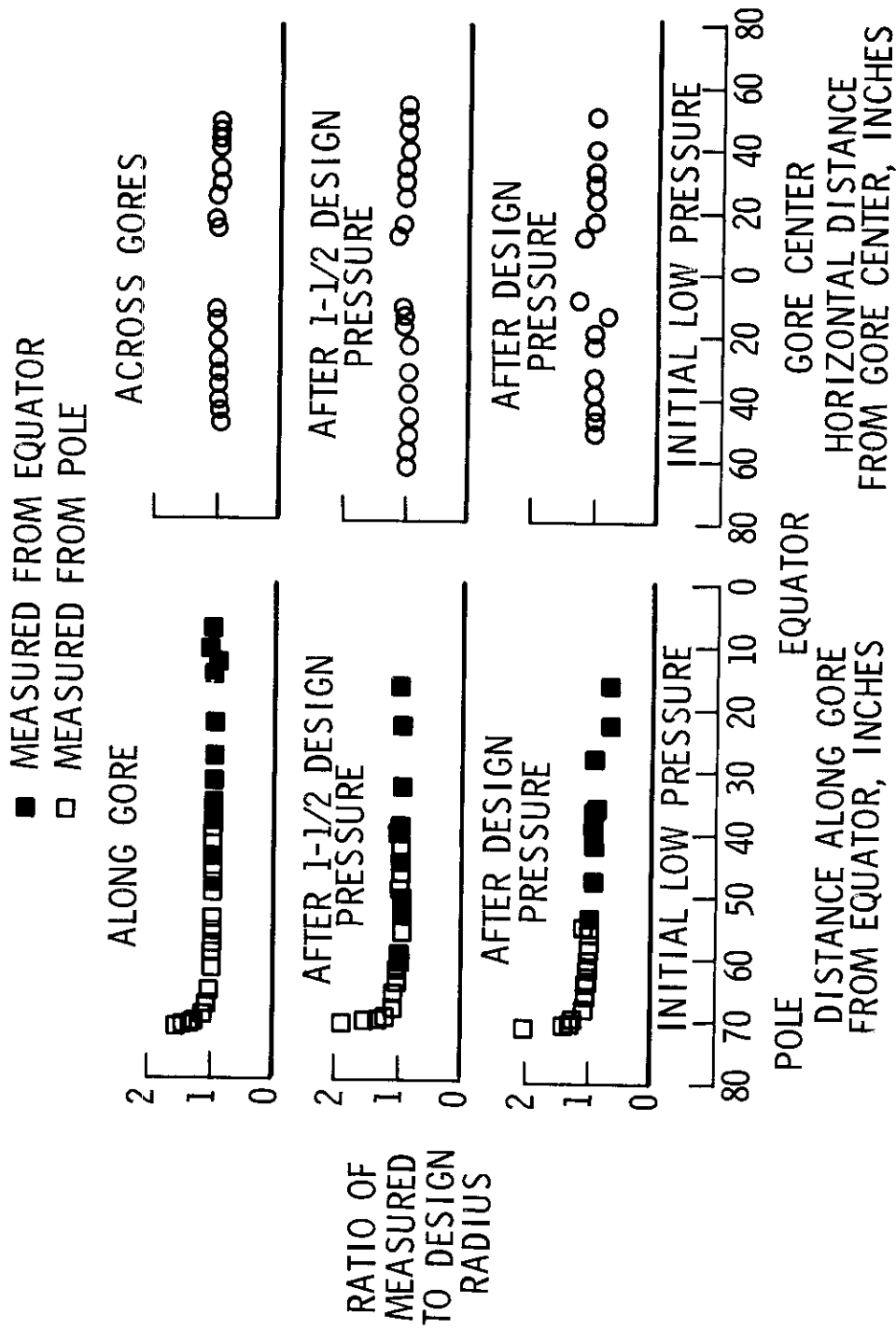


Figure 8.- Typical contour measurement plot.



NASA

Figure 9.- Ratio of measured to design radius of curvature before and after pressurization for 32-gore approximate sphere.